Dynamics of a Thermoreversible Transition between Cylindrical and Hexagonally Perforated Lamellar Mesophases

Chiajen Lai,† Yueh-Lin Loo,‡ and Richard A. Register*

Department of Chemical Engineering, Princeton University, Princeton, New Jersey 08544

Douglas H. Adamson

Princeton Institute for the Science and Technology of Materials, Princeton University, Princeton, New Jersey 08540

Received May 6, 2005; Revised Manuscript Received June 13, 2005

ABSTRACT: A polystyrene−poly(ethylene-*alt*-propylene) diblock copolymer, S/EP 7/13, exhibits a thermoreversible mesophase transition between low-temperature hexagonally perforated lamellae (HPL) and high-temperature hexagonally packed cylinders (C). The transformation process is accompanied by a 6% change in the principal spacing, yet oriented specimens retain their macroscopic orientation through the transition. The C → HPL transformation proceeds on a time scale of tens of minutes, at a rate which initially increases rapidly with undercooling relative to the order−order transition temperature. At deep undercoolings, the transformation rate slows due to a reduction in molecular mobility. By contrast, the HPL → C transformation occurs nearly 2 orders of magnitude more rapidly, a difference which is suggested to reflect the nature of the dominant fluctuation modes for the two structures.

Introduction

Transformations from one block copolymer mesophase to another—so-called order−order transitions (OOTs)—have been the subject of intense investigation over the past decade. Transitions between different equilibrium phases can be induced thermally, by varying the Flory interaction parameter χ at essentially constant block copolymer composition (volume fraction ϕ of one block), since boundaries dividing these phases are curved in a plot[1] of χN vs ϕ (where N is the copolymer's degree of polymerization). Thermoreversible transitions have been demonstrated experimentally between a body-centered-cubic packing of spheres (S) and hexagonally packed cylinders (C),[2−5] between the gyroid phase (G) and C,[6−9] and between lamellae (L) and hexagonally perforated lamellae (HPL).[10−12] In some cases, the transformation process has been followed in detail;[3,5,7,9] sigmoidal (Avrami-type) transformation kinetics were observed, suggesting a nucleation and growth process. Finally, in at least one case, the transformation rate was determined as a function of temperature and found to follow a simple Arrhenius dependence.[7]

However, thermoreversible transitions between layered phases (HPL or L) and C have received relatively little attention, principally because no system has been reported which produces such a thermoreversible OOT at a tractable rate. In a low-molecular-weight rod−coil diblock copolymer, Ryu et al.[13] recently observed transitions from L, to HPL, to tetragonally perforated lamellae, and finally to C upon heating; the last two of these transitions were shown to be thermoreversible and rapid. But for coil−coil diblock copolymers, a different progression of phases is expected. In the phase diagram calculated from self-consistent-field theory,[1] L and C border only at strong segregations, where the OOT dynamics are expected to be slow. Hajduk et al.[14] found a thermoreversible L ↔ C transition in a polystyrene−poly(ethylene-*co*-butene) diblock, and the transformation was indeed quite sluggish, with the C → L transition requiring days to complete. The L → C transition proceeded through an intermediate structure identified as sheets of cylinders lacking a hexagonal packing; the C → L transition proceeded without any signature of an intermediate structure.[14] There are also several reports of irreversible C → L[15] and L → C[16] transitions, corresponding to the relaxation of nonequilibrium structures formed through casting from a selective solvent. However, since such transitions start from structures very far from equilibrium, their relaxation pathways may differ significantly from those of order−order transitions between stable phases; moreover, the transformation rate will largely be governed by the polymer mobility (e.g., proximity to the upper glass transition temperature), rather than by thermodynamics (i.e., distance from T_{OOT}).

As for the HPL structure, it is believed to be metastable[17] relative to G; thus, when HPL is found, it is typically at weak segregations and at values of ϕ between those for L and C, where G is stable. G and C share a phase boundary, implying that thermally induced HPL → C transitions should be possible, though the reverse C → HPL transition might be problematic, with C → G occurring instead. Indeed, while HPL has been shown to convert to C upon heating in several bulk diblock copolymers,[18,19] the reversibility of this transition was not demonstrated. On the other hand, Wang and Lodge[8,9] reported a C → HPL transition following a deep temperature quench for a concentrated solution of a polystyrene−polyisoprene diblock in dibutyl phthalate. The HPL structure subsequently transformed to G, but this second transition was slow (hours), permitting the C → HPL transformation mechanism and kinetics (minutes) to be studied. Thermoreversibility of

† Present address: Bristol-Myers Squibb Pharmaceutical Research Institute, P.O. Box 191, New Brunswick, NJ 08903.

‡ Present address: Department of Chemical Engineering, The University of Texas at Austin, Austin, TX 78712.

* To whom correspondence should be addressed: e-mail register@princeton.edu.

10.1021/ma050953n CCC: $30.25
Published on Web 07/13/2005

this C ↔ HPL transition was not demonstrated directly, but is presumed since C is the stable high-temperature phase.

Here, we examine a thermoreversible HPL ↔ C transition in a bulk polystyrene−poly(ethylene-*alt*-propylene) diblock, S/EP 7/13. The phase diagram for S/EP diblock copolymers has been presented previously[20] and contains a substantial region where HPL is observed (denoted there as L′). Over this region of compositions and temperatures, HPL does not transform to G at any perceptible rate. For S/EP 7/13, an OOT from HPL (at low temperatures) to C (at high temperatures) occurs near 175 °C.[20] Here, we determine the transformation rate as a function of undercooling or superheating (vs T_{OOT}) and find a large asymmetry in the transformation rate, with HPL → C proceeding nearly 2 orders of magnitude faster than C → HPL. This asymmetry is discussed with regard to the epitaxial HPL ↔ C mechanism proposed previously.[8,9,21,22]

Experimental Section

The synthesis and molecular characterization of S/EP 7/13 have been described in detail previously.[20] Briefly, sequential anionic polymerization of styrene and then isoprene was employed, and the polyisoprene block selectively hydrogenated to EP. S/EP 7/13 has a polydispersity < 1.04, no detectable homopolymer, a weight-average molecular weight $M_w = 20.7$ kg/mol, and an EP volume fraction $\phi_{EP} = 0.709$ at 140 °C.

Three small-angle X-ray scattering (SAXS) systems were employed in this work. All kinetic measurements of the relatively slow C → HPL transition were conducted on unoriented specimens, using a compact Kratky camera with Cu Kα radiation from a sealed-tube generator. Scattering data were acquired with a one-dimensional position-sensitive detector (Braun OED-50M). SAXS at elevated temperature employed a custom-constructed hotstage with a temperature uniformity of ±1 °C;[23] satisfactory SAXS data could be acquired with 5 min time resolution. The data were reduced using previously reported procedures[24] to desmeared absolute intensity vs the magnitude of the momentum transfer vector $q \equiv (4\pi/\lambda) \sin \theta$, where θ is half the scattering angle and λ the radiation wavelength. The much faster HPL → C transition was examined on beamline 8.2 of the Synchrotron Radiation Source (Daresbury Laboratory, Warrington, UK),[25] with $\lambda = 0.154$ nm. SAXS patterns were acquired with 6 s time resolution, using a Daresbury quadrant detector. A Linkam DSC600 stage controlled the sample temperature to within ±0.05 °C. Finally, two-dimensional SAXS measurements[26,27] on oriented samples were conducted using Cu Kα X-rays from a sealed tube, a Statton (pinhole) camera, and Kodak image plates read with a Molecular Dynamics PhosphorImager SI. Measurements at elevated temperature employed the original Statton camera hotstage (W.H. Warhus, Inc.), retrofitted with a digital temperature controller to provide temperature stability within ±1 °C. Oriented specimens were prepared by planar extensional flow in a lubricated channel die.[28] The processed strip, ∼0.5 mm thick, was cut into pieces along the three orthogonal directions; these pieces were stacked together, taking care to match their orientations, to produce a total specimen thickness of ∼1.5 mm along the beam direction. After reaching the target temperature, the specimen was held for a minimum of 30 min to allow the morphology to stabilize; acquisition of the 2D SAXS pattern required 3 h.

Specimens for transmission electron microscopy (TEM) were prepared by heating 1 mm thick films of S/EP 7/13 in the Kratky camera, to either 120 °C (HPL) or 190 °C (C). SAXS patterns taken at the relevant temperature confirmed the desired structure, and subsequent patterns taken at room temperature confirmed that no morphological transformation occurred upon quenching. A portion of each film was then immersed in aqueous RuO_4 (0.5 wt %) overnight to selectively stain the S domains. After embedding in acrylic resin, thin sections were prepared by microtoming at room temperature and examined on a Zeiss 910 TEM in bright field.[29]

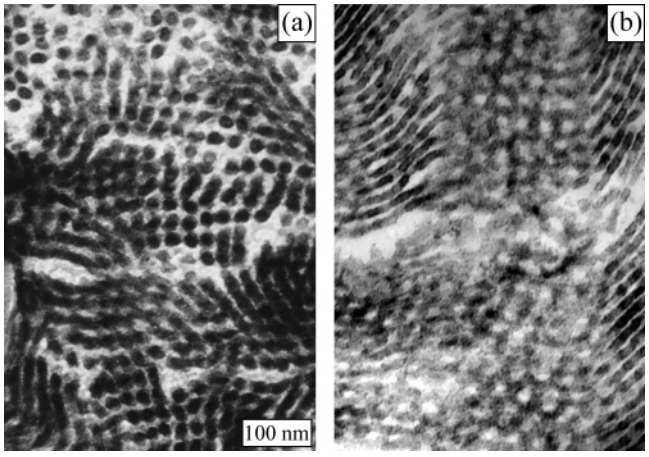

Figure 1. TEM images of S/EP 7/13; polystyrene domains are stained dark with RuO_4. (a) C phase, obtained by annealing at 190 °C. (b) HPL structure, obtained by annealing at 120 °C.

Results and Discussion

HPL and C Structures: Characteristics and Regions of Stability. TEM images of S/EP 7/13 are shown in Figure 1; the minority polystyrene block is stained dark with RuO_4. Panel (a) shows an image of the specimen quenched from 190 °C, where the C phase is stable.[20] Grains of cylinders with their axes roughly normal to the plane of the section, as well as some whose axes are inclined, are evident in the image. Panel (b) shows an image of the specimen quenched from 120 °C, where the HPL structure prevails.[20] The center portion of the image shows a region where the lamellar normal is roughly perpendicular to the section; uniform, circular domains of EP (light) perforating the S layers are evident. The edges of the image show regions where the lamellar normal lies roughly in the plane of the section; the perforations are evident from the regular modulation in thickness and darkness of the S layers. These features are similar to those seen in micrographs of the slightly less-asymmetric S/EP 9/14 (with $\phi_{EP} = 0.667$ at 140 °C), which forms a highly regular, ABCABC-stacked HPL structure.[12] However, the in-plane arrangement of the perforations (hexagonal vs disordered) and the stacking are unclear from the TEM image in Figure 1b and are better probed through SAXS.

Figure 2 shows high-resolution SAXS patterns of S/EP 7/13 at 170 °C (HPL) and 180 °C (C). The pattern at 180 °C is typical for hexagonally packed cylinders: a sharp primary peak at q^* (= 0.309 nm^{-1} here) and higher-order peaks at $\sqrt{3}q^*$, $\sqrt{7}q^*$, and $\sqrt{9}q^*$. (The structure factor peak at $\sqrt{4}q^*$ is absent due to coincidence with the cylinder form-factor node.[14]) The HPL SAXS pattern is less well-defined, showing only two strong reflections: a broad first-order peak at q^* (= 0.29 nm^{-1} here) and a relatively sharp higher-order peak at $2q^*$; a weak sharp peak at $3q^*$ can also be discerned. The inset to Figure 2 shows the SAXS pattern for the previously studied[12] S/EP 9/14, which forms a highly regular HPL structure with an ABCABC stacking; the peaks are labeled with corresponding ($h0l$) indices. Comparison of the HPL SAXS patterns for the two materials shows that the broad first-order peak observed for S/EP 7/13 is actually the superposition of three peaks: (1) the principal peak at q^*, due to the

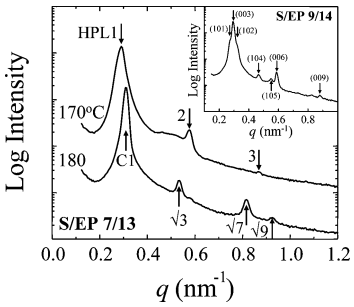

Figure 2. High-resolution SAXS profiles (logarithmic intensity scale) of S/EP 7/13, taken on Daresbury beamline 8.2. Top: HPL structure (at 170 °C), with arrows marking peaks resulting from the layer spacing; bottom: C phase (at 180 °C), with arrows indicating the positions of reflections characteristic of a hexagonal packing. Profiles are offset by a decade along the intensity axis for clarity. For comparison, the inset shows the SAXS profile of S/EP 9/14 at 260 °C, where it exhibits a highly regular HPL structure.[12] Arrows correspond to the positions of the indicated ($h0l$) reflections, for a regular ABCABC stacking of the perforations.

layer spacing (the (003) reflection in an ABCABC-stacked HPL structure), (2) a smaller peak at approximately $0.92q^*$ (the (101) reflection), and (3) a still smaller peak at approximately $1.09q^*$ (the (102) reflection). The broad but clearly discernible feature near $1.75q^*$ in S/EP 7/13 can be viewed as the superposition of the (104) and (105) reflections (at $1.59q^*$ and $1.88q^*$, for ABCABC stacking and $c/a = 2.24$);[12] such a feature has also been simulated by Hamley et al.[30] starting from a disordered arrangement of perforations. However, identification of these features is only possible because we have the SAXS pattern from the well-ordered S/EP 9/14 for comparison and because of the high flux and high resolution provided by the synchrotron source; at lower resolution, the SAXS pattern at 170 °C could easily be mistaken for that from an ordinary, unperforated L phase. Indeed, Hajduk et al.[17] noted that SAXS patterns from unsheared HPL specimens are typically indistinguishable from L. For S/EP 7/13, the emerging shoulders on either side of the main peak, as well as the broad feature near $1.75q^*$, indicate some regularity in the arrangement of the perforations, so we will continue to refer to the structure as HPL below, though clearly the perforations are not as highly ordered as in S/EP 9/14.

Figure 3 shows the evolution of the SAXS pattern for S/EP 7/13 on heating through the HPL → C transition, with a SAXS pattern shown every 10 °C. Panel (a) shows a three-dimensional plot; from the disappearance of the second-order HPL reflection, and the appearance of the $\sqrt{3}$ and $\sqrt{7}$ C reflections, the OOT occurs between 170 and 180 °C. Panel (b) shows how the first-order peak position changes during the heating ramp; by taking the temperature at which dq^*/dT is maximum, we assign $T_{OOT} = 175$ °C. The small breadth (ca. ±1 °C) of the transition is comparable to the temperature uniformity over the Kratky camera's slit length. Note that the OOT is accompanied by a substantial (6%) increase in q^*, indicating that the (10) interplanar spacing in the C structure is 6% smaller than the layer spacing in the HPL structure. Such a large change is surprising, since Wang and Lodge[9] found a near-epitaxial match (≈2% decrease in q^* on transformation from C to HPL) in their concentrated solution of a polystyrene−polyisoprene diblock.

Figure 4 demonstrates the thermoreversibility of the HPL ↔ C transition. Cycling the temperature repeatedly between 140 °C (HPL) and 180 °C (C), according to the temperature profile shown in the top panel, causes the structure to completely transform in <1 h. The SAXS peak shapes, positions, and intensities are fully recovered following a temperature jump or drop. None of our experiments showed any evidence of HPL transforming to G, even in samples annealed for several hours at a variety of temperatures. Thus, the HPL structure we see in S/EP 7/13 is stable for practical purposes (even if thermodynamically metastable relative to G[17]), which permits us to investigate the kinetics and mechanism of the HPL ↔ C transition in both directions.

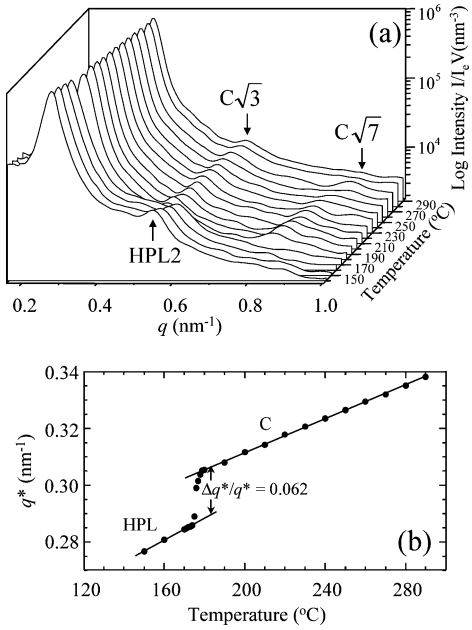

Figure 3. (a) Desmeared Kratky SAXS profiles for S/EP 7/13 (logarithmic intensity scale) during heating. At 170 °C and below, the structure is HPL, as evidenced by the two clear peaks in a q ratio of 1:2, as well as the broad feature near $1.75q^*$. At 180 °C and above, peaks at $q/q^* = \sqrt{3}$ and $\sqrt{7}$ are visible, characteristic of the C structure. (b) Position of the first-order peak (at q^*) during the heating process (30 min per step) from HPL to C. Note the sharp discontinuity at $T_{OOT} = 175$ °C.

HPL ↔ C Transition in Oriented Specimens. Flow alignment of block copolymers can be a great asset in elucidating the pathways of mesostructural transformations,[10] since it permits SAXS reflections to be resolved azimuthally as well as in q. Moreover, for the HPL structure, flow is often effective in producing a regular arrangement of the perforations, even when such regularity is absent in quiescent specimens.[17] We oriented samples of S/EP 7/13 via planar extensional flow in a lubricated channel die.[28] The three orthogonal directions are the flow direction (FD, direction of extension), loading direction (LD, direction of contraction), and constraint direction (CD, no net flow). Previous experiments[28] have shown that planar extension generally produces an alignment of cylinder axes along FD and lamellar normals along LD. Portions of the flow-aligned sample were cut in the three orthogonal directions for examination by SAXS, with the beam directed along FD, CD, or LD; note that each view necessarily corresponds to a different piece of material, though all were obtained from neighboring regions of the same flow-aligned strip. The results for a specimen flow-aligned at 150 °C (where the HPL structure prevails)

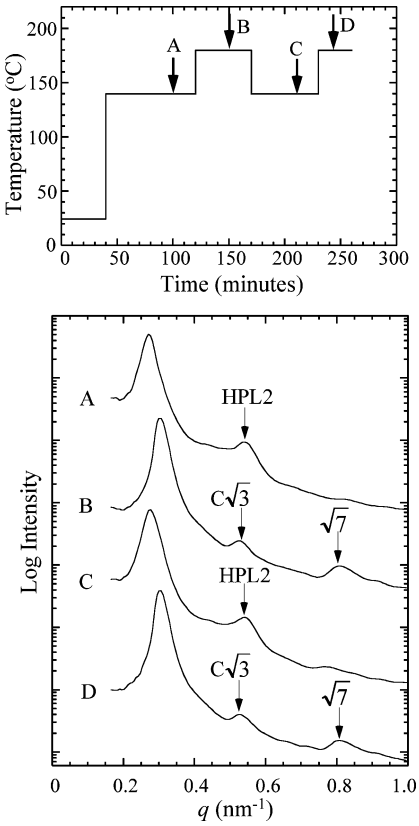

Figure 4. SAXS patterns (bottom) for S/EP 7/13 (logarithmic intensity scale, offset along the intensity axis for clarity) and corresponding temperature history (top), demonstrating complete thermoreversibility of the HPL ↔ C transition in <1 h. SAXS patterns A and C were acquired at 140 °C (HPL structure), while those at B and D were acquired at 180 °C (C phase).

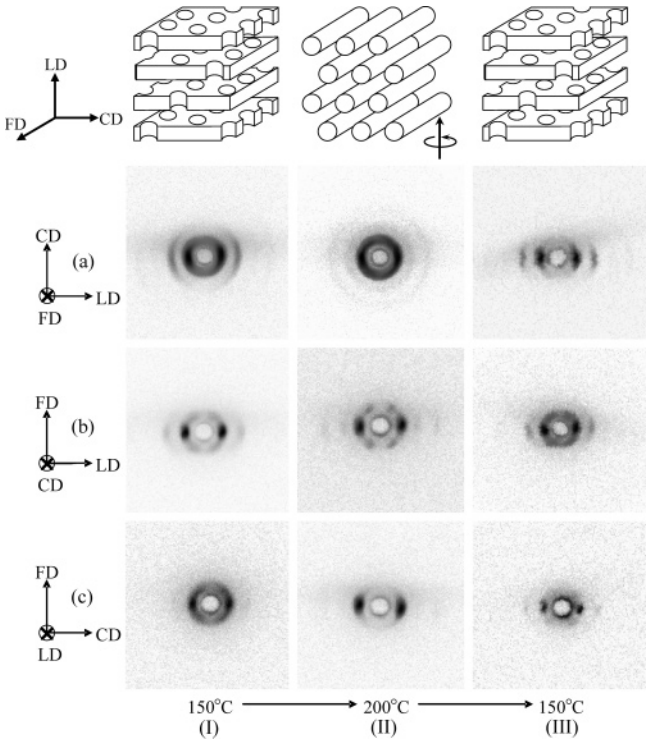

Figure 5. 3 × 3 matrix of 2D SAXS patterns for S/EP 7/13, flow-aligned at 150 °C, in the three orthogonal directions (beam along FD, CD, and LD in rows (a), (b), and (c), as indicated by the axes along the left margin). Column I: patterns after reheating from room temperature to 150 °C (HPL structure), the original processing temperature. Column II: patterns after heating further, to 200 °C (C phase). Column III: patterns after cooling from 200 °C back to 150 °C. Schematics along the top margin of the figure represent the structure at each temperature.

are shown in Figure 5. Column I shows the three orthogonal views of the as-aligned sample. With the beam directed along FD or CD, equatorial spots at q^* and $2q^*$ are observed, as expected for a lamellar structure. Moreover, the view along CD shows four off-axis spots inclined at 52° with respect to the equator and at a scattering angle slightly greater than q^*; these are the (102) reflections in the ABCABC-stacked HPL structure,[31,32] indicating that planar extensional flow is indeed effective in producing a highly regular arrangement of the perforations. Similar off-axis maxima are expected in the view along FD but cannot be resolved due to the larger azimuthal spread of the lamellar normals. Channel-die alignment typically yields some misorientation of the lamellar normals in the LD−CD plane, producing narrower arcs with the beam along CD than along FD.[28] Finally, the view along LD—with strong equatorial maxima and four weak off-equatorial maxima—results from a minor fraction of "perpendicular" perforated lamellae, with their normals aligned along CD.[6]

Heating the specimen to 200 °C transforms the morphology to C. Intuitively, we expect that the HPL → C transformation will occur by elongating and connecting the perforations to produce discrete cylinders with their axes lying in the plane of the original lamellae; this transformation pathway is also predicted theoretically.[21,22] Since even the ideal HPL structure is 6-fold symmetric about the lamellar normal, and our flow-aligned specimens are not perfect single crystals, this would be expected to produce a polygrain C structure, where all C axes lie in the FD/CD plane but with rotational disorder about LD. The view along CD (row b, column II) is consistent with this notion: two strong spots are observed along LD (where all grains contribute), with four weaker spots inclined at 60° relative to LD (where only grains whose cylinder axes are nearly aligned with CD contribute). The view along FD is also consistent with this idea, as it shows two strong spots along LD. However, the view along LD is a surprise: we anticipate a ring but observe arcs with strong maxima along CD. This indicates a strong preference for alignment of the cylinder axes along FD, as indicated schematically above column II, even though the HPL → C transformation occurs quiescently.

Subsequently cooling the specimens to 150 °C regenerates the HPL morphology. Moreover, the original orientation is also recovered, as evidenced by the similarity of the SAXS patterns in columns I and III. This, too, is a surprise, since we anticipate that the HPL structure will be formed by connecting adjacent cylinders periodically along their densest-packed (10) planes. The 6-fold symmetry of the C structure produces three sets of (10) planes, which would seem equally likely candidates to become the lamellar sheets in the HPL structure. This would give rise to six spots of equal intensity in the view along FD, yet spots are observed only on the equator, indicating a strong preference for alignment of the lamellar normals along LD, as indicated in the schematic above column III.

Similar "memory effects" have been seen in other OOTs, as discussed by Wang and Lodge,[9] who suggest

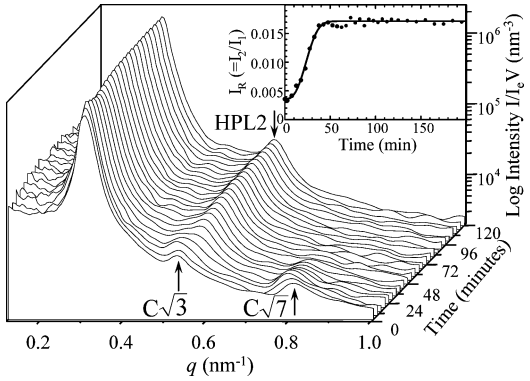

Figure 6. SAXS profiles (logarithmic intensity scale) for the time course of the C → HPL transformation, following a quench from 180 to 140 °C. The pattern at time = 0 was acquired just prior to the quench. Inset: peak intensity ratio I_R during the course of the transformation. The solid line represents an Avrami fit to the data (best-fit exponent $n = 3.0$).

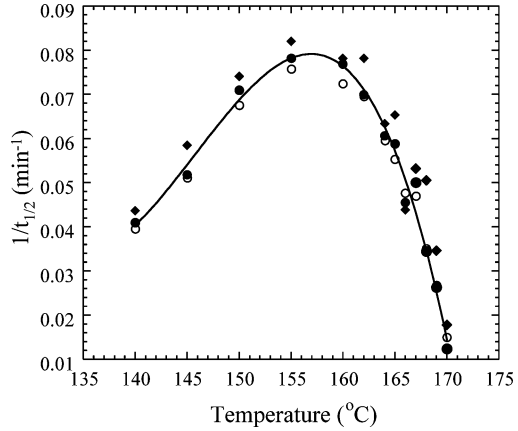

Figure 7. C → HPL transformation rate, as measured by the reciprocal of the transformation half-time ($t_{1/2}$), as a function of temperature following a quench from 180 °C. Half-times determined from I_R (●), A_R (○), and q^* (◆) are essentially identical.

that their origin may be small structural distortions resulting from imperfect epitaxy. For example, in the HPL → C transformation, such distortions would result in deviations from perfect hexagonal packing in the C phase, leading to a denser packing of cylinders along one particular set of (10) planes and thus providing a means to select this set of planes during the reverse C → HPL transformation. Unfortunately, the spots in the 2D patterns of Figure 5 are severely broadened by the instrumental resolution function, making any small deviations from perfect hexagonal symmetry in panel b-II impossible to detect. However, we note that the deviations from a true lattice match in this process are quite large: as can be seen from Figure 3, the change in q^* on heating from 150 to 200 °C is ∼13%, with half of the change due to the OOT at 175 °C and the other half to the general reduction in interdomain spacing as temperature increases (and χ decreases). Thus, changes in the domain spacing are relatively facile, suggesting that any distortions of the macrolattice which may be present immediately after the transformation should be quickly erased. As noted by Wang and Lodge,[9] the origin of this memory effect remains mysterious and warrants further investigation.

Kinetics of the HPL ↔ C OOT. Figure 6 shows time-resolved SAXS data for a specimen of S/EP 7/13 originally heated to 180 °C and then quenched to 140 °C (at time = 0). With increasing time at 140 °C, the higher-order C peaks at $\sqrt{3}$ and $\sqrt{7}q^*$ disappear, while the second-order reflection of the HPL structure (the (006) reflection for ABCABC stacking[12]) emerges at $2q^*$, as indicated by the arrows. As implied by Figure 3b, the primary peak position q^* also changes significantly, though this is difficult to discern in the 3D plot of Figure 6. The rate of the C → HPL transition can be quantified through the parameter $I_R \equiv I_2/I_1$, where I_2 is the intensity of the second-order peak for the HPL structure and I_1 is the intensity of the primary peak. The evolution of I_R with time is shown in the inset. The C → HPL transformation is adequately described by the Avrami equation:[33]

$$I_R = (I_{R0} - I_{R\infty}) \exp[-kt^n] + I_{R\infty} \qquad (1)$$

where t denotes the elapsed time at the target temperature, I_{R0} and $I_{R\infty}$ are the I_R values at $t = 0$ and $t \to \infty$, k is the rate constant, and n is the Avrami exponent. Experiments analogous to that in Figure 6 were conducted at target (quench) temperatures ranging from 140 to 170 °C; in all cases, the transformation kinetics were sigmoidal, with the best-fit n generally decreasing as the target temperature increased (undercooling decreased).[34] Thus, the transformation appears to proceed by nucleation and growth, and not by spinodal decomposition, even for undercoolings as deep as 35 °C.

The Avrami fits are also convenient for determining the half-time $t_{1/2}$ ($t = t_{1/2}$ when $I_R = (I_{R0} + I_{R\infty})/2$); $t_{1/2}$ is useful for comparing rates when the apparent exponent n changes with temperature. Besides I_R, two other parameters were tracked to quantify the progress of the transformation: a peak area ratio A_R ($\equiv A_2/A_1$), analogous to I_R, and the peak position q^*. Figure 7 shows reciprocal half-times obtained from these three quantities; there is no significant difference between the half-times from I_R and A_R, and those from q^* track quite well also. The latter is somewhat fortuitous: in principle, the observed first-order peak should consist of distinct peaks for HPL and C, at q^* values which differ by ∼6% (see Figure 3b). However, the first-order peak from the HPL structure is broad (see Figure 2), so the superposition of these two peaks appears as a single peak with a q^* value that varies continuously throughout the transformation.

Figure 7 shows that the rate initially increases very steeply as the undercooling is increased (temperature is decreased from T_{OOT} = 175 °C). However, each successive increment of undercooling increases the rate by a successively smaller factor: for example, increasing the undercooling from 5 to 6 °C nearly doubles the rate, but a further increase to 7 °C undercooling results in only a ≈40% increase in rate. This indicates that the kinetics are not Arrhenius-like; however, simple Arrhenius kinetics are not expected here, as the rate must rigorously go to zero at T_{OOT}. As the target temperature is further decreased, the transformation rate reaches a maximum (near 157 °C) and then enters a region where the rate actually decreases with a further decrease in temperature. This reduction in rate arises from a reduction in molecular mobility, especially as the glass transition of the polystyrene domains (measured as 65 °C in S/EP 7/13 by differential scanning calorimetry) is approached. A similar maximum in rate (minimum in half-time) has been observed in the disorder-to-order transition in polystyrene−polyisoprene diblock and triblock copolymers, for the same reason.[23]

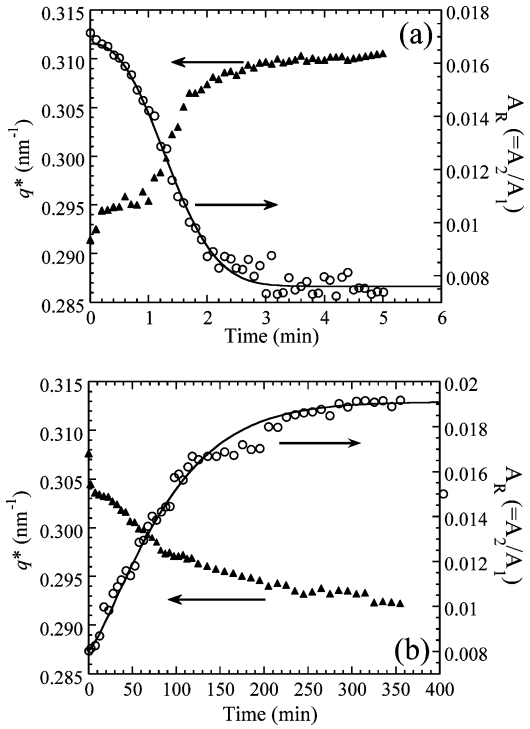

Figure 8. Comparison of the HPL → C and C → HPL transformations, each with an undercooling/superheating of 5 °C relative to T_{OOT} = 175 °C. Both A_R (○) and q^* (▲) are shown for each transformation; solid curves are the Avrami fits to the A_R data. (a) Jump from 170 to 180 °C, inducing the HPL → C transformation; $t_{1/2}$ = 1.3 min and Avrami exponent n = 2.4. (b) Drop from 180 to 170 °C, inducing the C → HPL transformation; $t_{1/2}$ = 75 min and Avrami exponent n = 1.3.

While the C → HPL transformation in S/EP 7/13 is easily studied with a laboratory SAXS system, preliminary measurements showed that the corresponding HPL → C transformation occurred in less than the 5 min necessary to acquire a SAXS pattern, even for small superheatings (5 °C). Consequently, the HPL → C transformation was tracked with synchrotron SAXS, following a jump from 170 to 180 °C; the initial and final SAXS patterns for this process are shown in Figure 2. The top panel of Figure 8 shows the progress of the transformation, as gauged through A_R and q^*; the kinetics are again sigmoidal, and the half-time extracted from A_R is 1.3 min. For comparison, results for the analogous C → HPL transformation—a quench from 180 to 170 °C, measured on the laboratory Kratky system—are shown in Figure 8b, with a half-time of 75 min. The degree of undercooling/superheating is the same in both cases—5 °C—and over this limited temperature range far from any glass transition, the molecular mobility is not expected to change greatly, yet the HPL → C transformation is over 50 times faster than the C → HPL transformation.

Such a large disparity in rates is surprising. Kim et al.[3] found the C → S and S → C transformation rates to be comparable (within a factor of 3, some of which can be attributed to differences in undercooling/superheating and molecular mobility). Floudas et al.[7] commented that the G → C transition proceeds much more slowly than C → G, but this difference in rate was not quantified. We speculate that the difference between the HPL → C and C → HPL transformation rates is a consequence of the dominant fluctuation modes for the two structures, as described theoretically by Laradji et al.[35] When the L phase is driven toward C, the dominant fluctuation mode leads to a perforated lamellar structure, which can then relax to C if one in-plane fluctuation mode dominates over the others. By contrast, when the C phase is driven toward L, the dominant fluctuation mode is a flattening of the cylinders along the (10) planes leading to rippled sheets when the cylinders touch. Thus, the dominant fluctuation mode for C does not facilitate the formation of an HPL structure, which could account for the relatively slow C → HPL kinetics.

Conclusions

The thermoreversible HPL ↔ C transformation process in a bulk diblock copolymer, S/EP 7/13, was effectively tracked by time-resolved SAXS over a broad range of transformation temperatures. Cooling transforms the C phase to HPL, rather than to gyroid (G) as in most prior reports; the HPL structure in S/EP 7/13 shows no evidence of transforming to G over the experimental time scale. Oriented specimens can be heated and cooled through the sequence HPL → C → HPL while retaining a memory of their original orientation, despite a 6% mismatch between the interlayer spacings in the two structures. In all cases, the time course of the C → HPL transformation satisfactorily fit the Avrami equation, implying a nucleation and growth process. The reverse HPL → C transformation also exhibits Avrami-type kinetics, but at a rate some 50 times faster than the C → HPL transformation, even for small excursions about T_{OOT}, where the segmental dynamics are little affected. We speculate that this rate asymmetry is a consequence of the favored fluctuation modes in the two structures; the HPL structure is easily converted to C, while the dominant fluctuations of the C structure favor an unperforated L structure, which S/EP 7/13 does not exhibit at any temperature.

Acknowledgment. This work was generously supported by the National Science Foundation through the Princeton Center for Complex Materials (DMR-9809483 and DMR-0213706) and the Polymers Program (DMR-9711436 and DMR-0220236). Beamtime at Daresbury was provided by the EPSRC, and the assistance of Professor Anthony J. Ryan and Dr. Ellen E. Heeley with the synchrotron experiments is gratefully acknowledged. C.L. thanks Dr. Shuyan Qi for stimulating discussions regarding mesophase transition mechanisms and Professor William B. Russel for helpful guidance at the outset of this project.

References and Notes

(1) Matsen, M. W.; Bates, F. S. *Macromolecules* **1996**, *29*, 1091.
(2) Sakurai, S.; Kawada, H.; Hashimoto, T.; Fetters, L. J. *Macromolecules* **1993**, *26*, 5796.
(3) Kim, J. K.; Lee, H. H.; Ree, M.; Lee, K.-B.; Park, Y. *Macromol. Chem. Phys.* **1998**, *199*, 641.
(4) Ryu, C. Y.; Vigild, M. E.; Lodge, T. P. *Phys. Rev. Lett.* **1998**, *81*, 5354.
(5) Krishnamoorti, R.; Modi, M. A.; Tse, M. F.; Wang, H.-C. *Macromolecules* **2000**, *33*, 3810.
(6) Vigild, M. E.; Almdal, K.; Mortensen, K.; Hamley, I. W.; Fairclough, J. P. A.; Ryan, A. J. *Macromolecules* **1998**, *31*, 5702.
(7) Floudas, G.; Ulrich, R.; Weisner, U.; Chu, B. *Europhys. Lett.* **2000**, *50*, 182.
(8) Wang, C.-Y.; Lodge, T. P. *Macromol. Rapid Commun.* **2002**, *23*, 49.
(9) Wang, C.-Y.; Lodge, T. P. *Macromolecules* **2002**, *35*, 6997.
(10) Almdal, K.; Koppi, K. A.; Bates, F. S.; Mortensen, K. *Macromolecules* **1992**, *25*, 1743.
(11) Mani, S.; Weiss, R. A.; Cantino, M. E.; Khairallah, L. H.; Hahn, S. F.; Williams, C. E. *Eur. Polym. J.* **2000**, *36*, 215.

(12) Loo, Y.-L.; Register, R. A.; Adamson, D. H.; Ryan, A. J. *Macromolecules* **2005**, *38*, 4947.
(13) Ryu, J.-H.; Oh, N.-K.; Zin, W.-C.; Lee, M. *J. Am. Chem. Soc.* **2004**, *126*, 3551.
(14) Hajduk, D. A.; Gruner, S. M.; Rangarajan, P.; Register, R. A.; Fetters, L. J.; Honeker, C.; Albalak, R. J.; Thomas, E. L. *Macromolecules* **1994**, *27*, 490.
(15) Sakurai, S.; Momii, T.; Taie, K.; Shibayama, M.; Nomura, S.; Hashimoto, T. *Macromolecules* **1993**, *26*, 485.
(16) Jeong, U.; Lee, H. H.; Yang, H.; Kim J. K.; Okamoto, S.; Aida, S.; Sakurai, S. *Macromolecules* **2003**, *36*, 1685.
(17) Hajduk, D. A.; Takenouchi, H.; Hillmyer, M. A.; Bates, F. S.; Vigild, M. E.; Almdal, K. *Macromolecules* **1997**, *30*, 3788.
(18) Hamley, I. W.; Koppi, K. A.; Rosedale, J. H.; Bates, F. S.; Almdal, K.; Mortensen, K. *Macromolecules* **1993**, *26*, 5959.
(19) Hamley, I. W.; Gehlsen, M. D.; Khandpur, A. K.; Koppi, K. A.; Rosedale, J. H.; Schulz, M. F.; Bates, F. S.; Almdal, K.; Mortensen, K. *J. Phys. II* **1994**, *4*, 2161.
(20) Lai, C.; Russel, W. B.; Register, R. A.; Marchand, G. R.; Adamson, D. H. *Macromolecules* **2000**, *33*, 3461.
(21) Qi, S.; Wang, Z.-G. *Phys. Rev. E* **1997**, *55*, 1682.
(22) Luo, K.; Yang, Y. *Polymer* **2004**, *45*, 6745.
(23) Adams, J. L.; Quiram, D. J.; Graessley, W. W.; Register, R. A.; Marchand, G. R. *Macromolecules* **1996**, *29*, 2929.
(24) Register, R. A.; Bell, T. R. *J. Polym. Sci., Part B: Polym. Phys.* **1992**, *30*, 569.
(25) Bras, W.; Derbyshire, G. E.; Devine, A.; Clark, S. M.; Cooke, J.; Komanschek, B. E.; Ryan, A. J. *J. Appl. Crystallogr.* **1995**, *28*, 26.
(26) Quiram, D. J.; Register, R. A.; Marchand, G. R.; Adamson, D. H. *Macromolecules* **1998**, *31*, 4891.
(27) Lee, L. B.-W.; Register, R. A.; Dean, D. M. *J. Polym. Sci., Part B: Polym. Phys.* **2005**, *43*, 97.
(28) Lee, H. H.; Register, R. A.; Hajduk, D. A.; Gruner, S. M. *Polym. Eng. Sci.* **1996**, *36*, 1414.
(29) Loo, Y.-L.; Register, R. A.; Adamson, D. H. *J. Polym. Sci., Part B: Polym. Phys.* **2000**, *38*, 2564.
(30) Hamley, I. W.; Castelletto, V.; Mykhaylyk, O. O.; Yang, Z.; May, R. P.; Zvelindovsky, A. V. *Langmuir* **2004**, *20*, 10785.
(31) Förster, S.; Khandpur, A. K.; Zhao, J.; Bates, F. S.; Hamley, I. W.; Ryan, A. J.; Bras, W. *Macromolecules* **1994**, *27*, 6922.
(32) Ahn, J.-H.; Zin, W.-C. *Macromolecules* **2000**, *33*, 641.
(33) Avrami, M. *J. Chem. Phys.* **1940**, *8*, 212.
(34) Lai, C. Ph.D. Thesis, Princeton University, 1999.
(35) Laradji, M.; Shi, A.-C.; Noolandi, J.; Desai, R. C. *Macromolecules* **1997**, *30*, 3242.

MA050953N